

# Effects of Walking Style and Symmetry on the Performance of Localization Algorithms for a Biped Humanoid Robot

Yukitoshi Minami Shiguematsu<sup>1</sup>, Martim Brandao<sup>2</sup>, and Atsuo Takanishi<sup>3</sup>

**Abstract**—Motivated by experiments showing that humans’ localization performance changes with walking parameters, in this paper we explore the effects of walking gait on biped humanoid localization. We focus on walking style (normal and gallop) and gait symmetry (one side slower), and we assess the performance of visual odometry (VO) and kinematic odometry algorithms for the robot’s localization. Changing the walking style from normal to gallop slightly improved the performance of the visual localization, which was related to a reduction in torques on the feet. Changing the gait temporal symmetry worsened the performance of the visual algorithms, which according to an analysis of inertial data, is related to an increase of mechanical vibrations and camera rotations. Both changes of gait style and symmetry decreased the performance of the kinematic localization, caused by the increase of vertical ground reaction forces, to which kinematic odometry is very sensitive. These observations support our claim that gait and footstep planning could be used to improve the performance of localization algorithms in the future.

**Index Terms** - Localization, ego-motion, visual odometry, kinematic odometry, humanoid robot, WABIAN-2R

## I. INTRODUCTION

The ability to self-localize in the environment is a crucial requirement for mobile robots. For humanoid robots, the ability to self-localize in the environment could greatly help them to become more useful in our daily life. One common way for the robot to self-localize is through odometry algorithms, i.e., the estimation of the robot’s change in position through the use of motion sensors, such as cameras, inertial measurement units (IMU), motor encoders, etc. These sensors can be used independently, as is the case of visual odometry (VO) algorithms, or their information can be combined to get better estimates, using algorithms based on probabilistic approaches, for instance.

Improving self-localization performance is a problem that can be tackled not only at the level of sensing and filtering but also motion planning. One approach to achieve this is to change the path a robot takes to a goal or the goals themselves in a way that optimizes said performance. This is called active localization, which refers to the act of partially

or fully controlling the motions of the robot to minimize the uncertainty and increase the efficiency and robustness of the estimation of its current pose [1], [2]. Humanoid robots could potentially use this approach also by changing inter-limb coordination or gait parameters while keeping the same base trajectory, to affect the camera motion and improve the robot’s localization performance.

The effect of walking style on self-localization systems has been analyzed in humans [3], [4], [5], [6], [7]. Humans modify their walking speed to improve their path integration with closed eyes [3]. However, current humanoid robot walking controllers and localization systems are built in ways fundamentally different from that of biological systems, and are not built with the purpose of achieving similar localization performances (i.e. similar relationship between walking speed and localization accuracy). Moreover, previous work with hexapod robots has found inconclusive and irregular variation of SLAM performance with gait parameters [8].

With the above in mind, the contribution of this paper is to answer the following questions regarding localization systems for biped humanoid robots:

- Does performance of such systems depend consistently and non-trivially with humanoid gait?
- What effects do different walking styles have on the performance of such systems?

The approach in this paper is data-driven, i.e., we do not try to predict localization performance from simplified mechanical, control, sensor, or environment models. Instead, we directly measure localization performance of the whole system, by using ground-truth data from motion capture on several experiments while varying the robot’s walking gait parameters. For this paper, we focus on gait style and symmetry, which are parameters that could potentially be used in the footstep planning phase of humanoid robot locomotion planning [9].

We describe this data-based approach and the data analysis in Section III. In Section IV we present the relationships found between localization performance for two different VO algorithms and one kinematic odometry algorithm and the mentioned gait parameters in our robotic platform. Also we discuss the possible explanations for the observed relationships quantitatively based on measurements of stepping impacts and inertial data. Finally we present our conclusions and future works in Section V.

## II. RELATED WORK

Self-localization for humanoid robots has been widely researched. In the case of VO algorithms, Stasse et al.

\*This study was conducted as part of the Research Institute for Science and Engineering, Waseda University, and as part of the humanoid project at the Humanoid Robotics Institute, Waseda University. It was also supported in part by the Program for Leading Graduate Schools, the Graduate Program for Embodiment Informatics of the Ministry of Education, Culture, Sports, Science and Technology of Japan (MEXT, Japan), by SolidWorks Japan K.K and Cybernet Systems Co.,Ltd. M. Brandao is funded by UK Research and Innovation and EPSRC, ORCA research hub (EP/R026173/1).

<sup>1</sup>Graduate School of Science and Engineering, Waseda University, Tokyo, Japan. [contact@takanishi.mech.waseda.ac.jp](mailto:contact@takanishi.mech.waseda.ac.jp)

<sup>2</sup>Oxford Robotics Institute, University of Oxford, UK.

<sup>3</sup>Department of Modern Mechanical Engineering and Humanoid Robotics Institute (HRI), Waseda University, Tokyo, Japan.

[10] proposed a real-time monocular Visual Simultaneous Localization and Mapping (VSLAM) algorithm taking into account robot kinematics from the walking pattern generator. In [11], an IMU based state estimation for a stereo based 3D SLAM is proposed, using measurements from the stereo VO and robot kinematics as updates for the Extended Kalman Filter (EKF).

For kinematics based approaches, Xinjilefu et al. [12] propose a decoupled estimation to reduce the computational cost but sacrificing some accuracy. Also, in [13], a bipedal robot state estimator is proposed, based on another originally designed for a quadruped robot [14]. These estimators make the filter update based on feet measurements. However none of the above analyzed the performance of their self-localization algorithms with walking parameters.

Regarding active localization for legged robots, [8] assessed the localization accuracy of a hexapod robot in different types of terrain changing the robot’s gait accordingly, using an RGB-D sensor.

More specifically for biped humanoid robots, active visual localization has been researched from different perspectives, as active localization to improve the interactions of the robot with its environment for object manipulation [15], an active vision system to estimate the location of objects while walking [16], or a task-oriented active vision system for a vision-guided bipedal walking [17]. None of the above assessed the effect of the walking motion itself on the performance of the robot’s localization, nor used this information to plan or modify the walking gait of the robot to obtain a better localization estimate.

From the biological point of view, humans plan their walking gait ahead in many situations, such as to keep stability in difficult situations like slippery terrains [5]. Humans also change gait parameters when there are problems with the sensory inputs, by decreasing walking speed or having a more backward leaning trunk posture when visual disturbances arise [6]. There is also evidence pointing out that modifying the walking speed makes humans underestimate distances when walking at slower speeds and overestimate at faster speeds [3], as well as walking cadence affecting the performance of path integration, achieving the best performance at about 2 Hz [7]. Also, the human odometer is sensitive to asymmetries in walking style [4].

### III. METHODOLOGY

As explained in Section I, in this paper we focus on the effects of walking style and walking symmetry on localization performance. We generated three different walking patterns, one normal walking pattern, one pattern we will call “gallop”, and one we will call “slow”, which will be described in the following Section. For all the patterns, the total walking distance was fixed to 1.5 m on a straight line, and the time to traverse that distance was kept inside the interval between 13.5 and 14.5 seconds. The step width was maintained constant at 0.08 m. Five runs were performed for each pattern. All patterns were executed on the robot by joint position control without any state estimation (i.e. assuming

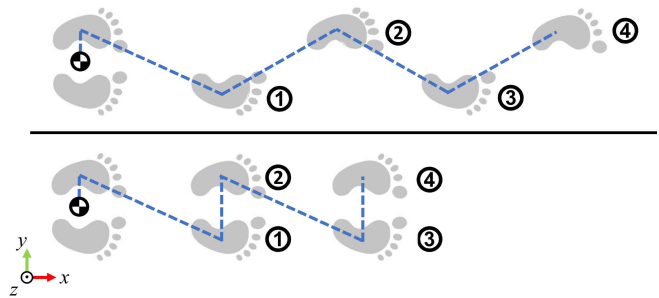


Fig. 1. Stepping order for the normal and slow (top), and gallop (bottom) walking patterns and approximate zero moment point (ZMP) reference (blue dashed lines).

the reference trajectory of the base was executed perfectly). The motion capture and robot’s joints, force, IMU and image data were stored and later analyzed.

#### A. Walking Gaits

As mentioned above, three walking patterns were tested:

- **Normal:** A walking pattern with a step length of 0.125 m and a reference walking cadence of 0.96 s/step, 0.06 seconds for double support phase and 0.9 seconds for single support phase.
- **Gallop:** A walking pattern that followed the rule ‘Step forward with the right foot, then bring the left foot into alignment with the right foot, pause and repeat’, as done in [4]. The step length was fixed to 0.25 m and the reference walking cadence was fixed to 0.96 s/step, 0.06 seconds for double support phase and 0.9 seconds for single support phase. (Fig. 1, bottom).
- **Slow:** A Normal walking pattern with a step length of 0.2 m, but a different reference walking cadence for each foot, one of 0.96 s/step (0.06 seconds for double support phase and 0.9 seconds for single support phase), and the other taking twice the time, i.e., 1.92 s/step (0.12 seconds for double support phase and 1.8 seconds for single support phase).

#### B. System Overview

For the experiments in this paper we used the biped humanoid robot WABIAN-2R [18] (Fig. 2), a 33 Degrees of Freedom (DoF) bipedal humanoid robot. For the visual input, we used a Matrix Vision mvBlueCOUGAR-X, a global shutter monocular camera, together with a low distortion wide angle lens of focal length 1.28 mm, a Field of View (FOV) of 125 deg and a distortion of 3%. The stream of images was set to 117 Hz, and the camera was mounted on the head of the robot (Fig. 3). For the ground truth measurements, a motion capture system OptiTrack V120:Trio at 120 fps was used, placing the photo-reflective markers on the camera to obtain the actual trajectory.

The different reference frames and transformations used for the experiments can be seen on Fig. 4. For the visual localization we use two main reference frames, the World frame, and  $C_t$ , the frame of the camera system at time

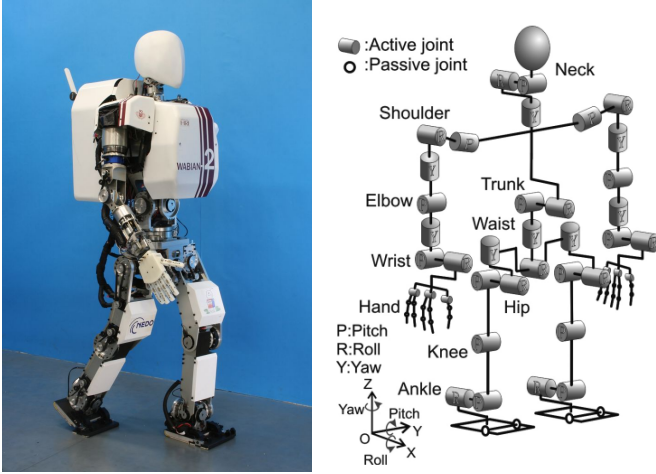


Fig. 2. Robotic platform WABIAN-2R (left) and DoF configuration (right).

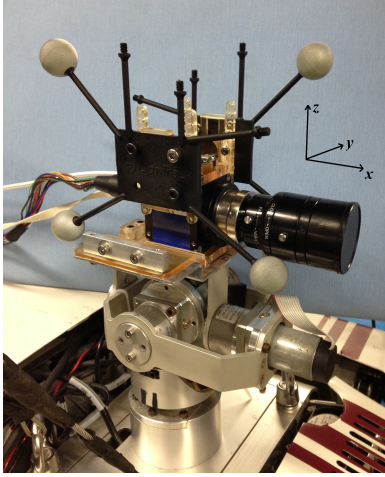


Fig. 3. Close-up of the head system used for localization and ground-truth (head, camera, reflective markers)

$t$ . Also, following the notation used in [19], we define  ${}^{(est)}T_{A_{t_i} \rightarrow B_{t_j}}$  as the transformation of frame  $B$  at time  $t_j$  relative to frame  $A$  at time  $t_i$ , calculated with the estimator  $est$ . The VO system tracks the motion of the camera system relative to its initial frame,  ${}^{(vo)}T_{C_{init} \rightarrow C_t}$ .

For the kinematic localization we use three main reference frames, the World frame,  $C_t$ , and  $F_t$ , the frame of the contact foot at time  $t$ . The kinematic odometry estimates the motion of the robot's head relative to the contact foot frame at each time stamp,  ${}^{(kin)}T_{F_t \rightarrow C_t}$ .

For both cases, the motion capture system tracks the camera system in the world frame,  ${}^{(gt)}T_{W \rightarrow C_t}$ .

For the robot's localization we used two visual odometry algorithms and one kinematic odometry algorithm. We tested a semi-direct VO algorithm, SVO 2.0 [20], and an indirect VO algorithm, ORB-SLAM2 [21], which we treated as a black boxes with default parameters. We fed the image stream and the intrinsic parameters of the camera, and extracted the estimated position and orientation of the camera.

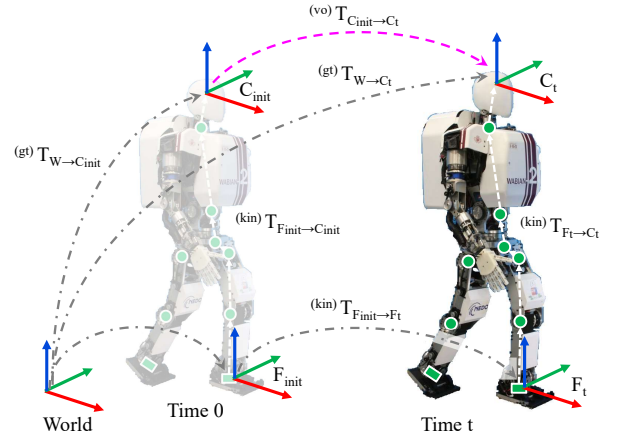


Fig. 4. Used coordinate frames.

For the kinematic odometry, we used an Extended Kalman Filter based approach for humanoid robots proposed in [22].

We also logged acceleration and angular velocity data at 200 Hz from one IMU mounted on the camera itself, as well as force and torque data from sensors placed on both feet, also at 200 Hz. This data was processed and analyzed to look for possible differences between different walking style and symmetry conditions. (Figs. 5, 6).

### C. Scale Extraction

To solve the scale ambiguity problem of monocular localization algorithms, we calculated the scale by comparing the estimated traveled distance of the camera after the first step, with the traveled distance obtained from the ground truth after the first step:

$$\lambda = \frac{{}^{(gt)}d_{first\ step}}{{}^{(vo)}d_{first\ step}} \quad (1)$$

where  $\lambda$  is the obtained scaling factor, and  $d_{first\ step}$  is the Euclidean distance between the initial position of the camera system and its position after the first step. We chose this method as it is one of the hypothesized ways in which humans try to calculate traveled distances while walking, using subtratal idiothetic cues, i.e., based on information about movement with respect to the ground or to inertial space [23].

## IV. DATA ANALYSIS

For the analysis of the localization performance using different gait styles, we focused on the absolute trajectory error (ATE), and the relative pose error (RPE) [24]. Both are calculated after aligning the trajectories using the method of Horn [25], which finds the rigid-body transformation corresponding to the least-squares solution that maps the estimated trajectory onto the ground truth trajectory in closed form.

The ATE is used to assess the global consistency of the estimated trajectory, by comparing the absolute distances between the estimated and the ground truth trajectories, after

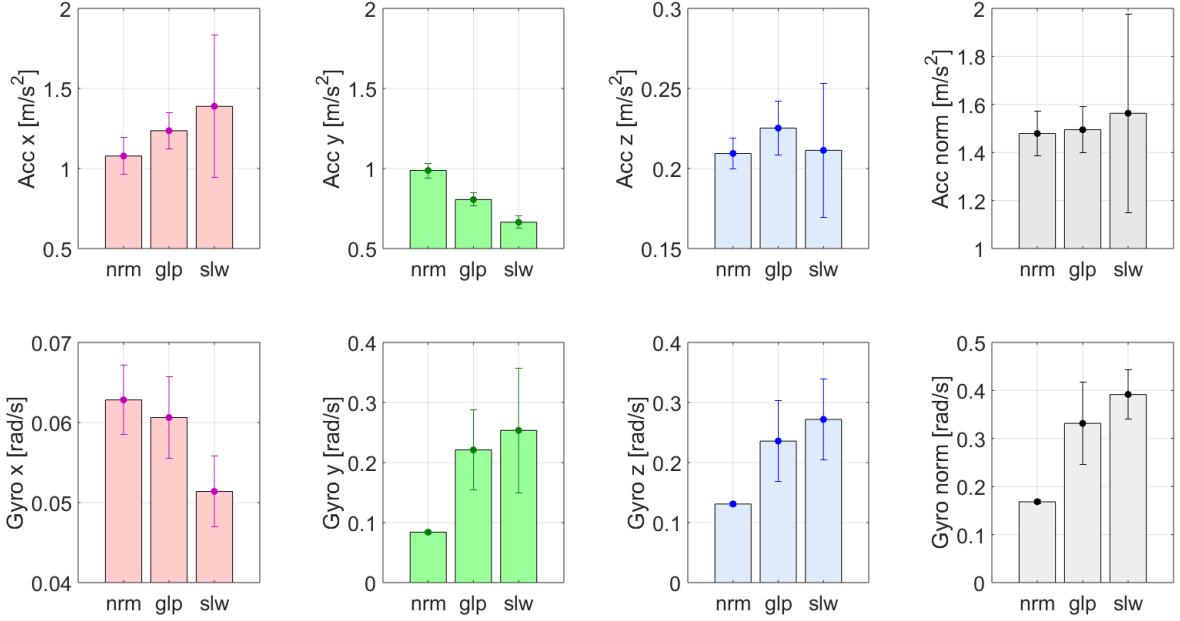


Fig. 5. RMS of the data from the accelerometer and gyroscope of the IMU mounted on the camera for normal (left), gallop (center) and slow (right). Markers with vertical error bars denote the average and standard deviations.

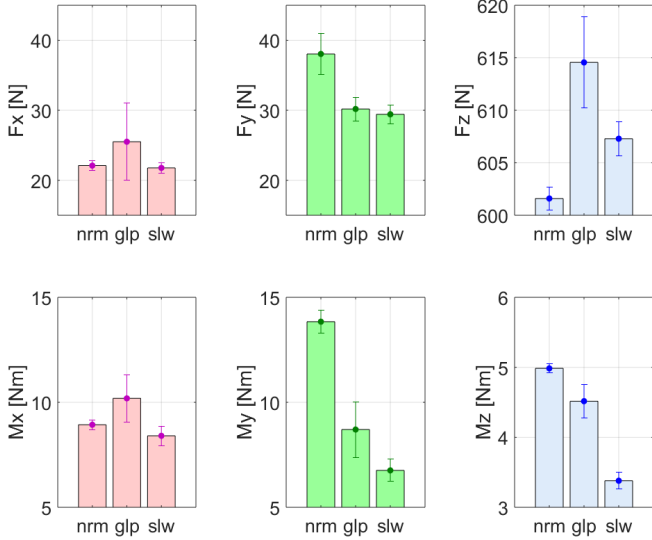


Fig. 6. RMS of the data from the F/T sensors on the robot’s feet for normal (left), gallop (center) and slow (right). Markers with vertical error bars denote the average and standard deviations.

both trajectories have been aligned (Fig. 7). We evaluated the root mean squared error over all time stamps of the translational components:

$$RMSE(ATE_t) = \left( \frac{1}{n} \sum_{i=1}^n \left\| {}^{(gt)}\mathbf{T}_{W \rightarrow C_i}^{-1} {}^{(vo)}\mathbf{T}_{W \rightarrow C_i} \right\|^2 \right)^{\frac{1}{2}} \quad (2)$$

On the other hand, the RPE is used to assess the drift between the estimated and ground truth trajectories. We set the time interval  $\Delta$  to 10 [ms], assuming that in this time

interval the motion is linear (Fig. 8). Similarly to the ATE, we evaluate the root mean squared error over all time stamps, with  $m = n - \Delta$ :

$$RPE_t = {}^{(gt)}\mathbf{T}_{C_t \rightarrow C_{t+\Delta}}^{-1} {}^{(vo)}\mathbf{T}_{C_t \rightarrow C_{t+\Delta}} \quad (3)$$

$$RMSE(RPE_t) = \left( \frac{1}{m} \sum_{i=1}^m \|RPE_i\|^2 \right)^{\frac{1}{2}} \quad (4)$$

#### A. Discussion

For both visual odometry algorithms, changing the walking style from normal to gallop slightly decreased the localization error (Fig. 7). This could be explained by the fact that both SVO 2.0 and ORB-SLAM2 show less localization error for a step length of 0.25  $m$ , i.e., the step length used for “gallop”, than for 0.125  $m$ , which is the one used for the normal walking gait (Fig. 9). Also, the moments around the  $y$  and  $z$  axes are smaller for “gallop” than for “normal” (Fig. 6), which could be another reason for the improvement on the localization performance.

On the other hand, changing from a normal to an asymmetrical gait (“slow” gait) increased both the error as well as the variance of the visual localization. From Fig. 9, and given that the step length for “slow” was 0.2  $m$ , we could expect the error for SVO 2.0 to be similar, and for ORB-SLAM2 to be smaller. However, ORB-SLAM2 is strongly affected by rotations, and in this case we can see high angular velocities for “slow” in the  $y$  and  $z$  axes (Fig. 5, lower row). In the case of SVO 2.0, the increase of localization errors could be caused by the high accelerations in the  $x$  axis, as well as the high variance of the accelerations on the  $z$  axis (Fig. 5, upper row).

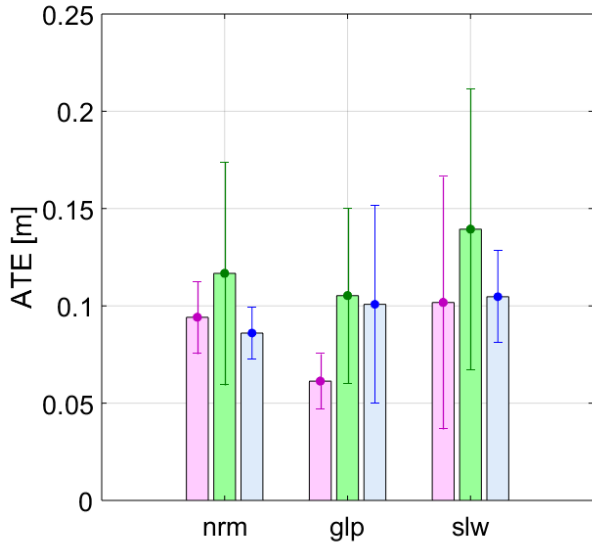


Fig. 7. ATE versus walking styles for SVO 2.0 (left, magenta), ORB-SLAM2 (center, green) and kinematic odometry (right, blue). Walking styles are normal (left collection), gallop (middle collection) and slow (right collection). Markers with vertical error bars denote the average and standard deviations.

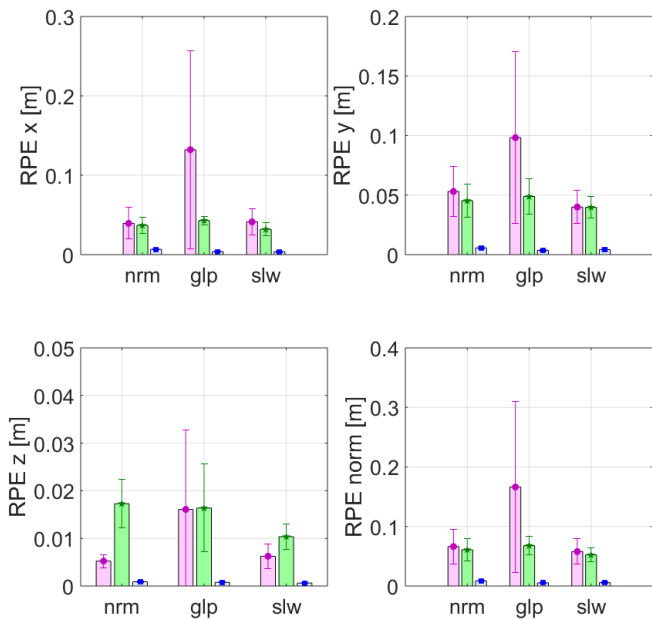


Fig. 8. RPE versus walking styles for SVO 2.0 (left, magenta), ORB-SLAM2 (center, green) and kinematic odometry (right, blue). Walking styles are normal (left collection), gallop (middle collection) and slow (right collection). Markers with vertical error bars denote the average and standard deviations.

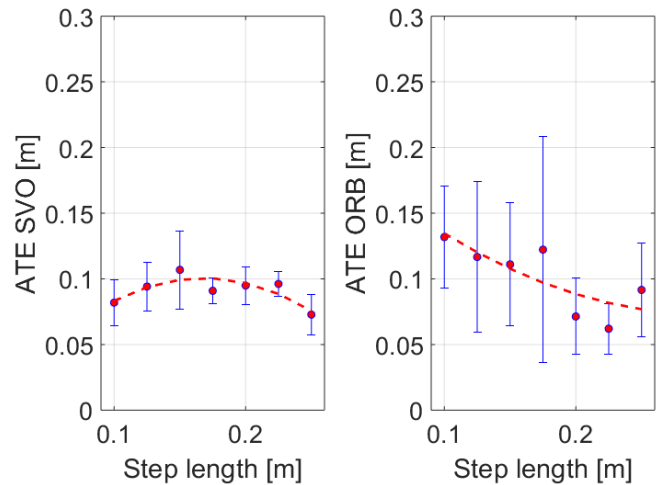


Fig. 9. ATE versus step length, for DSO, SVO 2.0 and ORB-SLAM2. Red dots with blue vertical error bars denote the average and standard deviations for each step length, while the red dashed lines are the fitted quadratic curves for the averages. Fitted quadratic curves were calculated using the *polyfit* function of MATLAB <sup>®</sup>.

It is interesting to note, however, that the moments around all the axes were the smallest for this asymmetrical gait (Fig. 6, lower row), but it did not seem to improve the performance of any localization algorithm.

For the kinematic odometry algorithm, changing both the style and symmetry increased the localization error slightly. This could be explained by the fact that both “gallop” and “slow” suffered more reaction forces on the vertical axis than normal walking. This could point to bigger impacts while walking, which affect the readings from the encoders as well as the monitoring of the contact foot switching, which is crucial for the kinematic odometry. It is also worth mentioning that the kinematic algorithm was the one with the least drift, as can be seen on Fig. 8, where the RPE is almost negligible compared to those of the visual algorithms.

## V. CONCLUSIONS AND FUTURE WORKS

### A. Conclusions

We performed a set of experiments with a biped humanoid robot for different walking styles and gait symmetry conditions, in order to find out whether these parameters would affect the performance of visual and/or kinematic localization. We tested a Semi-direct (SVO2.0) and an indirect (ORB-SLAM2) VO algorithms, as well as a kinematic odometry algorithm [22].

Using a gallop gait decreased the localization error for visual localization, which the data shows to be related to a decrease in the moments around  $y$  and  $z$ , caused either by the walking style itself, or because of the change in step length.

Eliminating the temporal symmetry of the walking gait increased the error of the visual localization, as well as its variance, even when from the step length point of view the error should have either remained or improved. For ORB-SLAM2 rotations could have affected the performance,

whereas for SVO 2.0 accelerations, most likely produced by vibrations during walking, affected its performance.

For the kinematic localization, both the gallop gait and the asymmetrical gait affected negatively the performance. Ground reaction forces on the vertical axis affected the most, as the kinematic odometry algorithm relies heavily on monitoring the which foot is in contact with the ground, which is the used to calculate the traveled distance from the kinematic chain.

### B. Future Works

As we observed a correlation between walking style and localization performance, we are planning to include these localization performance curves as cost functions within a footstep planner [9] such as to minimize localization error.

Regarding gait symmetry, in this work we focused on temporal asymmetry, but we are planning to explore other kinds of asymmetries, such as posture asymmetry.

Also, we are interested in exploring how the localization performance is influenced by other gait parameters such as stepping time, i.e. the duration of single and double support phases.

### REFERENCES

- [1] D. Fox, W. Burgard, and S. Thrun, "Active markov localization for mobile robots," *Robotics and Autonomous Systems*, vol. 25, no. 3-4, pp. 195-207, 1998.
- [2] G. Costante, C. Forster, J. Delmerico, P. Valigi, and D. Scaramuzza, "Perception-aware path planning," *arXiv preprint arXiv:1605.04151*, 2016.
- [3] J. Bredin, Y. Kerlirzin, and I. Isral, "Path integration: is there a difference between athletes and non-athletes?" *Experimental Brain Research*, vol. 167, no. 4, pp. 670-674, Dec. 2005.
- [4] M. T. Turvey, C. Romaniak-Gross, R. W. Isenhower, R. Arzamarski, S. Harrison, and C. Carello, "Human odometer is gait-symmetry specific," *Proceedings of the Royal Society B: Biological Sciences*, vol. 276, no. 1677, pp. 4309-4314, Dec. 2009.
- [5] R. Cham and M. S. Redfern, "Changes in gait when anticipating slippery floors," *Gait & Posture*, vol. 15, no. 2, pp. 159 - 171, 2002.
- [6] A. Hallemans, E. Ortibus, F. Meire, and P. Aerts, "Low vision affects dynamic stability of gait," *Gait & Posture*, vol. 32, no. 4, pp. 547-551, Oct. 2010.
- [7] H. S. Cohen and H. Sangi-Haghpeykar, "Walking speed and vestibular disorders in a path integration task," *Gait & Posture*, vol. 33, no. 2, pp. 211-213, Feb. 2011.
- [8] J. Faigl, "On localization and mapping with RGB-D sensor and hexapod walking robot in rough terrains," in *Systems, Man, and Cybernetics (SMC), 2016 IEEE International Conference on*. IEEE, 2016, pp. 002 273-002 278.
- [9] M. Brandao, K. Hashimoto, J. Santos-Victor, and A. Takanishi, "Optimizing energy consumption and preventing slips at the footstep planning level," in *15th IEEE-RAS International Conference on Humanoid Robots*, Nov 2015, pp. 1-7.
- [10] O. Stasse, A. J. Davison, R. Sellaouti, and K. Yokoi, "Real-time 3d slam for humanoid robot considering pattern generator information," in *2006 IEEE/RSJ International Conference on Intelligent Robots and Systems*. IEEE, 2006, pp. 348-355.
- [11] S. Ahn, S. Yoon, S. Hyung, N. Kwak, and K. S. Roh, "On-board odometry estimation for 3d vision-based SLAM of humanoid robot," in *Intelligent Robots and Systems (IROS), 2012 IEEE/RSJ International Conference on*. IEEE, 2012, pp. 4006-4012.
- [12] X. Xinjilefu, S. Feng, W. Huang, and C. G. Atkeson, "Decoupled state estimation for humanoids using full-body dynamics," in *Robotics and Automation (ICRA), 2014 IEEE International Conference on*. IEEE, 2014, pp. 195-201.
- [13] N. Rotella, M. Bloesch, L. Righetti, and S. Schaal, "State estimation for a humanoid robot," in *Intelligent Robots and Systems (IROS 2014), 2014 IEEE/RSJ International Conference on*. IEEE, 2014, pp. 952-958.
- [14] M. Bloesch, M. Hutter, M. A. Hoepflinger, S. Leutenegger, C. Gehring, C. D. Remy, and R. Siegwart, "State estimation for legged robots-consistent fusion of leg kinematics and IMU," *Robotics*, p. 17, 2013.
- [15] D. Gonzalez-Aguirre, M. Vollert, T. Asfour, and R. Dillmann, "Robust real-time 6d active visual localization for humanoid robots," in *Robotics and Automation (ICRA), 2014 IEEE International Conference on*. IEEE, 2014, pp. 2785-2791.
- [16] O. Lorch, J. F. Seara, K. H. Strobl, U. D. Hanebeck, and G. Schmidt, "Perception errors in vision guided walking: analysis, modeling, and filtering," in *Robotics and Automation, 2002. Proceedings. ICRA'02. IEEE International Conference on*, vol. 2. IEEE, 2002, pp. 2048-2053.
- [17] J. Seara and G. Schmidt, "Intelligent gaze control for vision-guided humanoid walking: methodological aspects," *Robotics and Autonomous Systems*, vol. 48, no. 4, pp. 231 - 248, 2004.
- [18] Y. Ogura, K. Shimomura, H. Kondo, A. Morishima, T. Okubo, S. Momoki, H. ok Lim, and A. Takanishi, "Human-like walking with knee stretched, heel-contact and toe-off motion by a humanoid robot," in *Intelligent Robots and Systems, 2006 IEEE/RSJ International Conference on*, Oct 2006, pp. 3976-3981.
- [19] R. Scona, S. Nobili, Y. R. Petillot, and M. Fallon, "Direct visual slam fusing proprioception for a humanoid robot," in *2017 IEEE/RSJ International Conference on Intelligent Robots and Systems (IROS)*, Sept 2017, pp. 1419-1426.
- [20] C. Forster, Z. Zhang, M. Gassner, M. Werlberger, and D. Scaramuzza, "Svo: Semidirect visual odometry for monocular and multicamera systems," *IEEE Transactions on Robotics*, vol. 33, no. 2, pp. 249-265, April 2017.
- [21] M. J. M. M. Mur-Artal, Raúl and J. D. Tardós, "ORB-SLAM: a versatile and accurate monocular SLAM system," *IEEE Transactions on Robotics*, vol. 31, no. 5, pp. 1147-1163, 2015.
- [22] M. F. Fallon, M. Antone, N. Roy, and S. Teller, "Drift-free humanoid state estimation fusing kinematic, inertial and LIDAR sensing," in *Humanoid Robots (Humanoids), 2014 14th IEEE-RAS International Conference on*. IEEE, 2014, pp. 112-119.
- [23] M.-L. Mittelstaedt and H. Mittelstaedt, "Idiothetic navigation in humans: estimation of path length," *Experimental Brain Research*, vol. 139, no. 3, pp. 318-332, Aug. 2001.
- [24] J. Sturm, N. Engelhard, F. Endres, W. Burgard, and D. Cremers, "A benchmark for the evaluation of rgb-d slam systems," in *2012 IEEE/RSJ International Conference on Intelligent Robots and Systems*, Oct 2012, pp. 573-580.
- [25] B. K. Horn, "Closed-form solution of absolute orientation using unit quaternions," *JOSA A*, vol. 4, no. 4, pp. 629-642, 1987.